Branched-Chain Amino Acid Catabolic Reprogramming in Heart Failure

Haipeng Sun[1, 2], Kristine C. Olson[3], Chen Gao[2], Domenick A. Prosdocimo[4], Meiyi Zhou[1], Zhihua Wang[2], Darwin Jeyaraj[4], Ji-Youn Youn[2], Shuxun Ren[2], Yunxia Liu[1], Christoph D. Rau[2], Svati Shah[5], Olga Ilkayeva[6], Wen-Jun Gui[7], Noelle S. William[7], R. Max Wynn[7], Christopher B. Newgard[6], Hua Cai[2], Xinshu Xiao[2], David T. Chuang[7], Paul Christian Schulze [8], Christopher Lynch[3], Mukesh K. Jain[4&], Yibin Wang[1,2&]

Supplementary Material

ON-LINE MATERIAL AND METHODS

Animals

. PP2Cm KO mice were backcrossed for more than 8 generations into a C57BL/6 background. Wildtype C57BL/6 mice and PP2Cm KO mice were housed at 22°C with a 12-hour light, 12-hour dark cycle with free access to water and standard chow. Studies were performed with male mice. All animal procedures were carried out in accordance with the guidelines and protocols approved by the University of California at Los Angeles Institutional Animal Care and Use Committee (IACUC).

Transverse Aortic Constriction

In mice, transverse aortic constriction (TAC) was performed as described {Gao, 2015 #808}in anesthetized (pentobarbital 60 mg/kg, IP) and ventilated mice (age 14–16 weeks) to induce hypertrophy and heart failure. After left anterolateral thoracotomy with blunt dissection through the intercostal muscles, aortic constriction was induced by ligating the transverse aorta around a 27 1/2-guage blunt needle using 6-0 silk suture. The needle was subsequently removed. Sham-operated mice underwent a similar surgical procedure without constriction of the aorta. All mice were maintained in the same environment with regular lab chow and water ad libitum. At the end of the experiments, animals were euthanized and the hearts and lungs were removed and weighed. Hearts were dissected and tissues were either immediately immersed into 4% buffered formaldehyde or quickly frozen in liquid nitrogen for further experiments.

BT-2 Treatment

Compound BT2 (3,6-dichlorobenzo[b]thiophene-2-carboxylic acid) was purchased from Sigma-Aldrich. Administration of BT2 was performed as previously described [1] except that animals (age ~8 weeks) were dosed daily by oral gavage at 40 mg/kg/day. Administration of BT2 started one week before TAC surgery and continued for 4 weeks post-TAC. Measurements of BCKD activity in mouse cardiac tissue and plasma BCKA/BCAA concentrations were performed as previously described [1].

Echocardiography

The mice were anesthetized and maintained with 1-2% isofluorane in 95% oxygen. Echocardiography was performed with a VisualSonics Vevo 770 (VisualSonics Inc, Toronto, Canada) equipped with a 30-MHz linear transducer. A parasternal short axis view was used to obtain M-mode images for analysis of fractional shortening, ejection fraction, and other cardiac parameters.

Mitochondrial Assay

The isolation of mitochondria to measure oxygen consumption was performed as described elsewhere [2]. Briefly, mitochondria were isolated from heart tissue and oxygen consumption was measured using an Ocean Optics fiber optic spectrofluorometer. Mitochondria (0.25 mg/ml) were added to the assay buffer (125 mM KCl, 10 mm HEPES-KOH, pH 7.4). The oxygen concentration in the buffer was continuously recorded via an Ocean Optics FOXY fiber optic oxygen sensor. Pyruvate, malate, and glutamate were added as free acids buffered with Tris (pH 7.4) for Complex I activity assay. Addition of 0.2mM ADP initiated oxygen consumption. NaCl or BCKA-Na mixture was added to the reaction system after the first pulse of ADP was consumed. Then the

second pulse of ADP was added. The oxygen consumption rate (OCR) was calculated with each ADP addition. The relative rate of oxygen consumption was calculated by dividing the OCR of second pulse of ADP by the OCR of the first pulse of ADP. Succinate was used for Complex II activity assay in presence of rotenone (1μM). The oxygen consumption rate (OCR) was calculated with each ADP addition. The presented data represented the average values of three independent experiments.

Western Blot Analysis

Proteins from heart tissue or cells were harvested in buffer (50mM HEPES [pH7.4], 150mM NaCl, 1% NP-40, 1mM EDTA, 1mM EGTA, 1mM glycerophosphate, 2.5mM sodium pyrophosphate 1mM Na3VO4, 20mM NaF, 1 mM phenylmethylsulfonyl fluoride, 1 μg/mL of aprotinin, leupeptin, and pepstatin). Samples were separated on 4-12% Bis-Tris gels (Invitrogen), and transferred onto a nitrocellulose blot (Amersham). The blot was probed with the indicated primary antibodies. Protein signals were detected using HRP conjugated secondary antibodies and enhanced chemiluminescence (ECL) western blotting detection regents (Pierce). Rabbit polyclonal antisera against the E1 and E2 subunits of BCKD complex is a kind gift from Dr. Yoshiharu Shimomura (Nagoya Institute of Technology). PP2Cm and phosphor-E1a antibodies were generated in the lab. The KLF15 primary antibody was purchased from Abcam.

Real-time RT-PCR and Microarray analysis

Total RNA was extracted from cells or tissues using Trizol Reagent (Invitrogen) according to the manufacturer's instructions. For neonatal mouse, 3-5 hearts were combined to extract RNA as one individual sample. Total RNA was reverse-transcribed into the first-strand cDNA using

the Superscript First-Strand Synthesis Kit (Invitrogen). Then, cDNA transcripts were quantified by the Step-One Plus Real-Time PCR System (ABI) using SYBR Green (ABI). 18sRNA were used for normalization except where indicated. PCR primer information is available upon request. The cDNA from wildtype and PP2Cm deficient mice was applied to Illumina MouseRef-8 v2.0 Expression BeadChips at the UCLA DNA Microarray Core Facility for whole-genome expression profiling. The data were analyzed with BeadStudio Gene Expression Module v3.4 program.

Bioinformatics Analysis

The transcriptomes of sham and failing mouse hearts [3] were analyzed using the Database for Annotation, Visualization, and Integrated Discovery (DAVID) (http://david.abcc.ncifcrf.gov). The lists of genes showing either up-regulation (782 genes) or down-regulation (653 genes) in failing hearts were separately entered into the DAVID and subjected to Functional Annotation Chart analysis with a EASE score of 0.05 using the KEGG pathway database. KEGG pathway tool was utilized through DAVID online tools to visually map down-regulated genes involved in BCAA degradation pathway in failing heart.

To predict upstream regulators of target genes, the down-regulated gene list (653 genes) was analysed using Ingenuity Pathway Analysis (IPA) Software (http://www.ingenuity.com). A Fisher's Exact Test p-value is calculated to assess the significance of enrichment.

Expression constructs, cell culture, transient transfection and luciferase Assay

Mouse KLF15 cDNA was generated from heart mRNA, inserted into the pFLAG-CMV-4 expression vector, and used to generate adenovirus [4]. Utilizing the NCBI GenBank, we identified the genomic sequence of mouse PP2Cm (*Ppm1k*). We amplified five proximal 5' regions (-468, -

412, -296, -254 to +20 bp relative to transcript start site, respectively) by PCR. Promoter PCR product was cloned into a firefly luciferase reporter pGL3-Basic vector (Promega, Madison, WI) to drive luciferase expression (PP2Cm-luc). The site-specific deletion was accomplished with the Agilent QuikChange XL site directed mutagenesis kit. Neonatal rat ventricular myocytes (NRVM) were isolated and cultured as previously described[5]. HeLa cell lines were maintained in DMEM (Invitrogen) supplemented with 10% fetal bovine serum, 2 mM L-glutamine, 100U/mL penicillin, and 100μg/ml streptomycin. Transient transfections were performed with the use of Lipofectamine 2000 reagent (Invitrogen). HeLa cells were seeded into 12 well plates at a density of 2×10^5 cells per well the day before transfection. For each well of cells 0.2 μg of the promoter constructs were co-transfected with 0.02 μg of the pSV40-Renilla vectors. The transfected cells were collected after transfection 48 hours. Luciferase activities were measured with the Dual-Luciferase Reporter Assay System (Promenade). To normalize for transfection efficiency, the promoter activity was expressed as the ratio of firefly activity to renilla activity. For each construct, more than three independent experiments were performed in triplicate.

Chromatin immunoprecipitation (ChIP) assay

Neonatal Rat Ventricular Myocytes (NRVM) ($4.0*10^7$) were mock or FLAG-KLF15 infected with adenovirus. 48 hr post infection, cells were cross-linked with 1% formaldehyde for 10min at room temperature. ChIP analysis was performed using SimpleChIP Enzymatic Chromatin IP Kit (Cell Signaling) according to the manufacture's protocol. Briefly, cross linking was terminated by adding glycine into cells for 5min at room temperature. Cells were harvested by PBS/PMSF and chromatin DNA was extracted. Following Micrococcal nuclease treatment, chromatin DNA was further sheared by sonication. Immuno-precipitation was performed using

Normal Rabbit IgG (Santa Cruz) or DYKDDDDK antibody (Cell Signaling) with ChIP Grade Protein G Magnetic Beads overnight. Following immune-precipitation, magnetic beads were washed with low salt buffer and high salt buffer according to the protocol, and the cross-linking was reversed by proteinase K digestion at 65 degree for 2hr. The eluted DNA was further purified using column provided in SimpleChIP Enzymatic Chromatin IP Kit. PCR was performed to detect enrichment of rat PP2Cm promoter region. For PP2Cm, forward primer sequence is 5'ACAAATTAAGACTAAAAAGT3' and reverse primer sequence is 5'CCCACAGGAACTAGTCAAGG3'. PCR products were separated using agarose gel electrophoresis and visualized. IgG was used as negative control for ChIP specificity.

Measurement of BCAA and BCKA concentrations in hearts

Mice on normal chow diet were either fasted for 6 hours or overnight followed with a high protein diet (40%, Teklad) feeding for two hours before tissue collection. BCKA level in KLF15 knockout heart was measured in mice fasted for 48 hours. Human left ventricular RNA samples were obtained as previously described[6]. In brief, myocardial specimens were collected before and after left ventricular assisted device (LVAD) implantation and explantation as a bridge to transplantation for end-stage HF patients. Control heart samples were obtained from non-failing hearts as previously described[6]. The use of all mouse and human samples was approved by the Institutional Review Board of Columbia University and Case Western Reserve University (IRB-AAAE7393). Freeze clamped mouse hearts were crushed with a metal mortar and pestle that was maintained at the temperature of liquid nitrogen. The powdered tissue was transferred to a tared tube, the weight recorded, and then processed with perchloric acid as previously described[7]. A ratio of 300 μl perchloric acid per 100 mg of tissue was used. The aliquotted perchloric acid

supernatant was stored at -80ºC until further assay. For BCAA determinations, a 20 µl perchloric acid supernatant aliquot of the mouse heart was thawed and neutralized with 0.25*M* MOPS-3*M* KOH buffer for analysis of free amino acids in the heart. The amino acids were derivatized and extracted as previously described using internal and external standards[8]. The samples were analyzed using a Waters Synapt HDMS hybrid QTOF with Ion Mobility. BCKA measurements were performed as described elsewhere[9]. Briefly, the perchloric acid heart supernatants were derivatized by o-phenylenediamine (OPD), extracted with ethyl acetate, and dried down in glass tubes in an unheated vacuum centrifuge. Following drying, the ketoacids were reconstituted in 200mM ammonium acetate, pH 6.8, and analyzed using a Shimadzu ultra-fast liquid chromatography (UFLC) 20ADXR LC system in-line with an AB-Sciex 5600 TripleTOF Q-TOF mass spectrometer (MS). Both instruments used in this analysis were housed in the Penn State College of Medicine Macromolecular Core Facility. BCKA concentration were measured and normalized to the weight of tissue. For human heart result, statistical analyses were performed with Student's t-test after log transforming the data.

BCKA Measurements in mouse Plasma: The method published by Olson, et al [9] was followed with modification. Briefly, plasma was cleared of proteins by adding an equal volume of methanol, followed by two rounds of centrifugation. The supernatant was lyophilized and re-suspended in distilled water (dH20). Stock solutions of each keto acid were prepared in dH20 and stored at -80C until they were used once and not refrozen. 10 ng of [^{13}C] KIV was added to each vial of sample and standard which were then derivatized with freshly prepared O-phenylenediamine (OPD) and extracted twice with ethyl acetate as described [9]. The pure organic phase was transferred to an eppendorf tube and dried under mild heat (40°C). The samples were re-suspended

in 50:50 MeOH:5 mM NH4 acetate and analyzed by LC-MS/MS using a Sciex 3200 Q-Trap coupled to a Shimadzu Prominence LC. An Agilent C18 XDB 5 micron packing column (50 X 4.6 mm) was used for chromatography with the following conditions: Buffer A: 5 mM NH4 acetate, Buffer B: methanol, 0 - 2.0 min 50% B, 2.0 - 2.5 min gradient to 100% B, 2.5 - 3.5 min 100% B, 3.5 - 3.6 min gradient to 50% B, 3.6 - 4.6 min 50% B. The derivatized keto acids were detected with the mass spectrometer in positive MRM (multiple reaction monitoring) mode using the following transitions: KIC 203.1 to 161.1 (retention time: 2.91 min); KIV 189.145 to 119.2 (retention time 2.84 min); KMV 203.065 to 174.2 (retention time 2.99 min); [^{13}C] KIV 194.109 to 120.1 (retention time: 2.84 min).

Human cohort for BCAA/BCKA measurements

One hundred forty one subjects with no history of diabetes were selected from the CATHGEN bio-repository for ketoacid analysis based on cardiomyopathy phenotype. This study was approved by the Duke University Institutional Review Board. Heart failure (n=91) cases were defined as those having left ventricular ejection fraction (LVEF) less than or equal to 30%, no history of heart transplantation, no significant valvular disease, with or without history of myocardial infarction (MI), and New York Heart Association (NYHA) Functional Classification of 2 or greater. The control group (n=50) was composed of those with LVEF greater than or equal to 55%, no coronary vessels occluded greater than or equal to 50%, no history of MI, no history of percutaneous coronary intervention (PCI), no history of coronary artery bypass grafting (CABG), no history of congestive heart failure or heart transplantation, and no significant valvular heart disease.

Electron spin resonance measurement of superoxide production

Freshly isolated hearts were placed into chilled modified Krebs/HEPES buffer (composition in mmol/l: 99.01 NaCl, 4.69 KCl, 2.50 $CaCl_2$, 1.20 $MgSO_4$, 1.03 KH_2PO_4, 25.0 $NaHCO_3$, 20.0 Na-HEPES, and 5.6 glucose [pH 7.4]), cleaned of excessive adventitial tissue. The homogenates from heart tissues were prepared by homogenizing with a pestle (50 strokes) in fresh homogenization buffer (50 mmol/L of Tris-HCl, [pH 7.4] 0.1 mmol/L of EDTA, 0.1 mmol/L of EGTA) containing protease inhibitor cocktail and centrifuged at 800 g for 10 min. After centrifugation, supernatants were collected and then subjected for protein assay. The specific superoxide ($O_2^{\bullet-}$) spin trap methoxycarbonyl-2,2,5,5-tetramethyl-pyrrolidine (CMH, 1mmol/L, Alexis) solution was prepared freshly in nitrogen gas bubbled Krebs/HEPEs buffer containing diethyldithiocarbamic acid (DETC, 5 μmol/L Sigma) and deferoxamine (25 μmol/L, Sigma). Homogenates (15 μg protein) was then mixed with the spin trap solution in the presence or absence of 100 units of SOD (manganese containing enzyme, Sigma) and loaded into a glass capillary (Fisher Scientific). For analysis of $O_2^{\bullet-}$ signal ($CM^{\bullet}$ formed after trapping $O_2^{\bullet-}$), the capillary was immediately loaded in an e-Scan electron spin resonance (ESR) spectrophotometer (Bruker Biospin, Germany). The ESR settings used were static-field, 3484 sweep width, 9.00 G (1 G = 0.1 mT); microwave frequency, 9.748660 GHz; microwave power 21.02 mW; modulation amplitude, 2470 mG; resolution in X, 512, number of X-scan, 10; and receiver gain, 1000. Data was presented as fold change versus WT. The superoxide production in isolated mitochondria was performed following a similar protocol except using an assay buffer containing 250mM sucrose, 10mM HEPES, 10mM Tris-HCl (pH7.4), and 4mM ADP.

Metabolomic analysis of heart tissue

The global metabolomic analysis was carried out by Metabolon, Inc. (Durham, NC) using heart tissues from PP2Cm KO and wildtype male mice at 14-16 weeks of age. Briefly, all samples were quickly frozen in liquid nitrogen and maintained at -80oC until processed. Samples were prepared using the automated MicroLab STAR® system from Hamilton Company. Several types of controls were analyzed in concert with the experimental samples. The LC-MS portion of the platform was based on a Waters ACQUITY ultra-performance liquid chromatography (UPLC) and a Thermo-Finnigan LTQ mass spectrometer operated at nominal mass resolution, which consisted of an electrospray ionization (ESI) source and linear ion-trap (LIT) mass analyzer. The samples destined for analysis by GC-MS were dried under vacuum prior to being derivatized under dried nitrogen using bistrimethyl-silyltrifluoroacetamide. Derivatized samples were separated on a 5% diphenyl / 95% dimethyl polysiloxane fused silica column and analyzed on a Thermo-Finnigan Trace DSQ fast-scanning single-quadrupole mass spectrometer using electron impact ionization (EI) and operated at unit mass resolving power. Raw data was extracted, peak-identified and QC processed using Metabolon's hardware and software. Peaks were quantified using area-under-the-curve. A collection of information interpretation and visualization tools for use by data analysts. Welch's two-sample t-test is used to test whether two unknown means are different from two independent populations. Principal component analysis (PCA) was used to visualize how individual samples in the cohort of wildtype and PP2Cm KO hearts differ from each other. The metabolites contributing the greatest to the differences among the two groups were determined in a random forest (RF) analysis. To determine which metabolites make the largest contribution to the classification, the "Mean Decrease Accuracy" is computed.

Statistics:

Unless otherwise specified, statistical analyses to compare two groups were performed with either the Student's t-test or Wilcoxon Rank Sum test (when $n < 5$ or in which the variances distributions differed based on Bartlett test). When more than two groups were analyzed, standard ANOVA followed by Newman-Keuls test was performed when $n > 5$ for all groups and passed by the Bartlett test of homogeneity of variances. Otherwise, Kruskal-Wallis test followed by Dunn's multiple comparison test was performed.

Presented values are mean with standard deviation or SEM (standard error of the mean). For repeated measurements over time as shown in longitudinal echocardiograph analysis, Linear Mixed Effect Model test using lmerTest package in R obtained from an on-line source was performed (Alexandra Kuznetsova, Per Bruun Brockhoff and Rune Haubo Bojesen Christensen (2015). lmerTest: Tests in Linear Mixed Effects Models. R package version 2.0-29. http://CRAN.R-project.org/package=lmerTest). A repeated measures linear model was fitted for echocardiograph parameters such as LVIDs and FS using animal ID as a random effect and day, group and group*day as fixed effects. A p value of less than 0.05 was considered statistically significant.

References cited in Methods:

1. Tso S-C, Gui W-J, Wu C-Y, Chuang JL, Qi X, Skvorak KJ, Dorko K, Wallace AL, Morlock LK, Lee BH, Hutson SM, Strom SC, Williams NS, Tambar UK, Wynn RM and Chuang DT. Benzothiophene Carboxylate Derivatives as Novel Allosteric Inhibitors of Branched-chain α-Ketoacid Dehydrogenase Kinase. *Journal of Biological Chemistry*. 2014;289:20583-20593.

2. Korge P, Yang L, Yang J-H, Wang Y, Qu Z and Weiss JN. Protective Role of Transient Pore Openings in Calcium Handling by Cardiac Mitochondria. *Journal of Biological Chemistry*. 2011;286:34851-34857.

3. Lee J-H, Gao C, Peng G, Greer C, Ren S, Wang Y and Xiao X. Analysis of Transcriptome Complexity Through RNA Sequencing in Normal and Failing Murine Hearts / Novelty and Significance. *Circulation Research*. 2011;109:1332-1341.

4. Fisch S, Gray S, Heymans S, Haldar SM, Wang B, Pfister O, Cui L, Kumar A, Lin Z, Sen-Banerjee S, Das H, Petersen CA, Mende U, Burleigh BA, Zhu Y, Pinto YM, Liao R and Jain MK. Kruppel-like factor 15 is a regulator of cardiomyocyte hypertrophy. *Proc Natl Acad Sci U S A*. 2007;104:7074-9.

5. Prosdocimo DA, Anand P, Liao X, Zhu H, Shelkay S, Artero-Calderon P, Zhang L, Kirsh J, Moore D, Rosca MG, Vazquez E, Kerner J, Akat KM, Williams Z, Zhao J, Fujioka H, Tuschl T, Bai X, Schulze PC, Hoppel CL, Jain MK and Haldar SM. Kruppel-like factor 15 is a critical regulator of cardiac lipid metabolism. *The Journal of biological chemistry*. 2014;289:5914-24.

6. Chokshi A, Drosatos K, Cheema FH, Ji R, Khawaja T, Yu S, Kato T, Khan R, Takayama H, Knoll R, Milting H, Chung CS, Jorde U, Naka Y, Mancini DM, Goldberg IJ and Schulze PC. Ventricular assist device implantation corrects myocardial lipotoxicity, reverses insulin resistance, and normalizes cardiac metabolism in patients with advanced heart failure. *Circulation*.

2012;125:2844-53.

7. Lynch CJ, Fox H, Hazen SA, Stanley BA, Dodgson S and Lanoue KF. Role of hepatic carbonic anhydrase in de novo lipogenesis. *The Biochemical journal*. 1995;310 (Pt 1):197-202.

8. Wilson GJ, Layman DK, Moulton CJ, Norton LE, Anthony TG, Proud CG, Rupassara SI and Garlick PJ. Leucine or carbohydrate supplementation reduces AMPK and eEF2 phosphorylation and extends postprandial muscle protein synthesis in rats. *American journal of physiology Endocrinology and metabolism*. 2011;301:E1236-42.

9. Olson KC, Chen G and Lynch CJ. Quantification of branched-chain keto acids in tissue by ultra fast liquid chromatography-mass spectrometry. *Anal Biochem*. 2013;439:116-22.

SUPPLEMENTAL DATA:

FIGURE LEGEND:

Supplemental Table S1. The top 25 KEGG pathways identified by DAVID.

Supplemental Table S2. The 25 down-regulated genes were identified and mapped into BCAA catabolism pathway by KEGG (Kyoto Encyclopedia of Genes and Genomes).

Supplemental Table S3. The top 10 proteins identified by Upstream Regulator Analysis of IPA with the list of genes down-regulated in failing heart.

Supplemental Figure S1. A. The densitometric values of the bands in Figure 1C were analyzed. The densitometric value of each protein was normalized to GAPDH and presented as fold change versus Sham (n=3 in each group). The data represented the average values with standard deviation of three bands with p value labeled. B, Western blotting result of BCAA catabolic enzymes with GAPDH as loading control. The densitometric value of phosphorylated BCKDE1a was compared to that of total BCKDHE1a and the ratio was shown on top of the panels.

Supplemental Figure S2. Individual BCAA concentration in tissues from normal (Sham, n=10) and failing (Failure, n=7) murine hearts was measured and normalized to the weight of tissue. Error bars represent SEM.

Supplemental Figure S3. Individual BCKA concentration in plasma from human with normal (Ctrl, n=50) or failing (Failure, n=91) hearts was measured. Error bars represent SEM. ∗, $p < 0.05$

compared to control.

Supplemental Figure S4. Individual BCAA concentration in tissues from normal (Ctrl, n=3) and failing (Failure, n=9) human hearts was measured and normalized to the weight of tissue. Error bars represent SEM.

Supplemental Figure S5. A, Real-time RT-PCR results of genes using mRNA from HeLa cells with (KLF15, n=3) or without (Vector, n=3) KLF15 overexpression. Y axis represents relative mRNA level. The data represented the average values with standard deviation of three samples. ∗, $p < 0.05$ compared to vector control. B, Luciferase assay result of PP2Cm promoter-luciferase in HeLa cells co-transfected with either KLF15 or corresponding empty vector. 486bp, the 486bp promoter of PP2Cm; 486bpDD, the 486bp promoter with two GC-rich sites deleted. The data represented the average values with standard deviation of triplicate samples from one experiment representative of three independent experiments. ∗, $p < 0.05$ compared to same promoter without KLF15 overexpression. #, $p<0.05$ compared to 468bp promoter with KLF15 overexpression.

Supplemental Figure S6. A, The densitometric values of the bands in Figure 34B were analyzed. The densitometric value of each protein was normalized to GAPDH. The data represented the average values of relative densitometry with standard deviation of four hearts. *, $p<0.05$ compared to WT control. B, Real-time RT-PCR result of KLF15 gene using mRNA from normal (Sham, n=3) and failing (Failure, n=3) heart induced by pressure overload. KLF15 mRNA level was normalized to 18sRNA. The data represented the average values with standard deviation of three hearts. ∗, $p < 0.05$ compared to control.

Supplemental Figure S7. A, Individual BCAA concentration in tissues from PP2Cm knockout (KO, n=5) and wildtype (WT, n=5) mouse heart were measured with mass spectrometer and normalized to weight of tissue. Error bars represent SEM. *, $p<0.05$. B, Gene expression was examined by microarray using RNA from PP2Cm knockout (KO, n=3) and wildtype (WT, n=3) mouse heart. The data was presented as fold change versus WT. ∗, $p<0.05$.

Supplemental Figure S8. Time course for Ejection Fraction (%EF), left ventricular internal dimension at diastole (LVIDd), left ventricular posterior wall thickness at diastole (LVPWd), and left ventricular posterior wall thickness at systole (LVPWs) from TAC WT (n=11-15) and PP2Cm KO mice (n = 9-13). The X-axis show the time in weeks after surgery. *, $p<0.05$ compared to WT.

Supplemental Figure S9. A, Oxygen consumption in mitochondria isolated from wildtype hearts in absence or presence of BCKA-Na (500μM each of KIC, KIV, KMV mixed). NaCl (1.5mM) was used as control. Y axis: oxygen concentration (ppm) in assay buffer. The assay was completed in ~12 minutes. B, Relative oxygen consumption rate in the absence or presence of BCKA calculated based on results in A (n=3 in each group).

Supplemental Figure S10. Deletion of PP2Cm resulted in significant global perturbations in cardiac metabolism. A, Random Forest Confusion Matrix. Random Forest classification using named metabolites detected in heart tissue of wildtype and PP2Cm KO mice resulted in a predictive accuracy of 100%. B, Metabolomic analysis showed higher level of glucose, glycolytic intermediates, glucose-derived sugars such as fructose, and malate in PP2Cm deficient heart (red,

n=7) compared to that in wildtype heart (blue, n=8) at baseline. Statistical analyses were performed with Welch's two-sample t-test. $p<0.05$ for all shown compounds.

Supplemental Figure S11. Inhibition of BCKDK by BT2 reduced plasma BCAA level. Individual BCAA concentration in plasma from wildtype and PP2Cm-KO (n=4-6) mice treated without (vehicle, veh group) or with BT2 (BT2 group). Error bars represent SEM. Statistical analyses were performed with Student's t-test to compare the values of two groups. *, $p<0.05$ compare to KO Veh group.

Supplemental Figure S12. Inhibition of BCKDK by BT2 preserves cardiac function. A. Left ventricular internal dimension at diastole (LVIDd), **B.** Left ventricle pastier wall thickness at systole (LVPWs) and **C**. diastole (LVPWd) from mice following sham or post-TAC surgery at 4 weeks, treated with or without BT2 (n=6-8 in each group). Error bars represent SEM. Statistical analyses were performed with One-Way ANOVA followed by Newman-Keuls test for **A and B**, or Kruskal-Wallis test followed by Dunn's multiple comparison test for **C**. *, $p<0.05$ between two groups.

Supplemental Table S1. The top 25 KEGG pathways identified by DAVID.

Term	Count	P Value	Fold Enrichment	Bonferroni	Benjamini	FDR (%)
mmu00280:Valine, leucine and isoleucine degradation	24	1.81E-21	13.859903	2.64E-19	2.64E-19	2.15E-18
mmu00640:Propanoate metabolism	16	2.34E-14	14.167901	3.42E-12	1.71E-12	2.78E-11
mmu00071:Fatty acid metabolism	16	3.16E-11	9.4452675	4.61E-09	1.54E-09	3.75E-08
mmu00650:Butanoate metabolism	10	6.14E-06	7.1796797	8.96E-04	2.24E-04	0.007295
mmu05012:Parkinson's disease	18	7.82E-06	3.5952381	0.0011406	2.28E-04	0.009291
mmu00380:Tryptophan metabolism	10	1.22E-05	6.6412037	0.0017841	2.98E-04	0.014536
mmu00190:Oxidative phosphorylation	17	2.37E-05	3.4738604	0.0034471	4.93E-04	0.028108
mmu00250:Alanine, aspartate and glutamate metabolism	8	9.17E-05	7.0839506	0.0132963	0.0016718	0.108912
mmu00982:Drug metabolism	12	9.38E-05	4.2503704	0.0135966	0.0015199	0.111386
mmu00480:Glutathione metabolism	10	1.11E-04	5.1086182	0.0161105	0.0016229	0.132136
mmu05010:Alzheimer's disease	19	1.40E-04	2.7732499	0.0201837	0.0018519	0.165858
mmu00980:Metabolism of xenobiotics by cytochrome P450	10	7.10E-04	4.0249719	0.0984886	0.008603	0.840523
mmu00410:beta-Alanine metabolism	6	0.001101	7.2449495	0.1486025	0.0122988	1.301148
mmu05016:Huntington's disease	17	0.001282	2.4677697	0.1708507	0.0132934	1.513677
mmu00062:Fatty acid elongation in mitochondria	4	0.002527	13.282407	0.3088142	0.0243224	2.96208
mmu00010:Glycolysis / Gluconeogenesis	9	0.003635	3.5159314	0.4123981	0.0326855	4.236249
mmu00310:Lysine degradation	7	0.003869	4.5354562	0.4322189	0.0327471	4.503388
mmu00620:Pyruvate metabolism	7	0.003869	4.5354562	0.4322189	0.0327471	4.503388
mmu00020:Citrate cycle (TCA cycle)	6	0.005402	5.1415771	0.5465242	0.042983	6.23512
mmu04260:Cardiac muscle contraction	9	0.008382	3.0651709	0.7073951	0.0626332	9.5205
mmu03320:PPAR signaling pathway	9	0.009034	3.0263713	0.734205	0.0641045	10.22559
mmu00330:Arginine and proline metabolism	7	0.013628	3.5085604	0.8651147	0.0909877	15.04856
mmu00130:Ubiquinone and other terpenoid-quinone biosynthesis	3	0.025914	11.384921	0.9783617	0.1599052	26.80674
mmu04920:Adipocytokine signaling pathway	7	0.038583	2.7754284	0.9968004	0.2210204	37.35432
mmu00051:Fructose and mannose metabolism	5	0.048199	3.5898398	0.9992625	0.2595595	44.40883

Supplemental Table S2. The 25 down-regulated genes were identified and mapped into BCAA catabolism pathway by KEGG (Kyoto Encyclopedia of Genes and Genomes).

Gene symbol	Fold decrease in failing heart	Description
Abat	1.57	4-aminobutyrate aminotransferase
Acaa2	2.11	acetyl-Coenzyme A acyltransferase 2
Acadm	1.84	acyl-Coenzyme A dehydrogenase, medium chain
Acadsb	1.51	acyl-Coenzyme A dehydrogenase, short/branched chain
Acat1	1.54	acetyl-Coenzyme A acetyltransferase 1
Aldh2	1.68	aldehyde dehydrogenase 2, mitochondrial
Aldh6a1	1.84	aldehyde dehydrogenase family 6, subfamily A1
Aox1	2.63	aldehyde oxidase 1
Bckdha	1.88	branched chain ketoacid dehydrogenase E1, alpha polypeptide
Bckdhb	1.76	branched chain ketoacid dehydrogenase E1, beta polypeptide
Dbt	1.98	dihydrolipoamide branched chain transacylase E2
Dld	1.55	dihydrolipoamide dehydrogenase
Ehhadh	1.58	enoyl-Coenzyme A, hydratase/3-hydroxyacyl Coenzyme A dehydrogenase
Hadh	1.72	hydroxyacyl-Coenzyme A dehydrogenase
Hadha	1.85	hydroxyacyl-Coenzyme A dehydrogenase/3-ketoacyl-Coenzyme A thiolase/enoyl-Coenzyme A hydratase
Hadhb	1.81	predicted gene 13910; similar to Hydroxyacyl-Coenzyme A dehydrogenase/3-ketoacyl-Coenzyme A thiolase/enoyl-Coenzyme A hydratase (trifunctional protein), beta subunit
Hibadh	1.55	predicted gene 11225; 3-hydroxyisobutyrate dehydrogenase
Hmgcs2	2.29	3-hydroxy-3-methylglutaryl-Coenzyme A synthase 2
Ivd	1.77	isovaleryl coenzyme A dehydrogenase
Mccc1	1.56	methylcrotonoyl-Coenzyme A carboxylase 1 (alpha)
Mccc2	1.57	methylcrotonoyl-Coenzyme A carboxylase 2 (beta)
Mcee	1.54	methylmalonyl CoA epimerase
Mut	1.63	methylmalonyl-Coenzyme A mutase Mus musculus
Pcca	1.61	propionyl-Coenzyme A carboxylase, alpha polypeptide
Ppm1k	2.20	protein phosphatase 1K (PP2C domain containing)

Supplemental Table S3. The top 10 proteins identified by Upstream Regulator Analysis of IPA with the list of genes down-regulated in failing heart.

Upstream Regulator	Molecule Type	p-value of overlap	Target molecules in dataset
MAP4K4	kinase	1.31E-17	ACAA2,ACACB,ACADVL,ALDH4A1,BCKDHB,CCBL2,COQ3,DHRS4,DLD,GCDH,GOT1,HADH,HADHA,HADHB,IVD,LDHB,MLXIPL,NDUFA5,NDUFS1,PEX11A,PHYH,PIGO,PLA2G12A,PXMP2,SLC2A4,SUCLG1
KLF15	transcription regulator	1.90E-15	ACADM,ACADVL,Acot1,ACSS1,CPT2,DECR1,DGAT2,EHHADH,HADHA,HADHB,MLYCD,PXMP2,SLC25A20,SLC27A1,SLC2A4,UCP3
PPARA	ligand-dependent nuclear receptor	5.77E-15	ABCD3,ACAA2,ACADM,ACADVL,ACAT1,Acot1,ACOT2,ACSL1,ALDH2,ALDOB,C3,CPT2,DECR1,ECH1,ECI1,EHHADH,FDFT1,FITM1,GPT,Gsta4,GSTK1,Gstt1,HADH,HADHA,HADHB,HMGCS2,HSD17B11,KHK,LGALS4,MGST1,MLYCD,MT-CO2,PAQR9,PEX11A,PLIN5,PPARA,RETSAT,SELENBP1,SLC25A20,SLC27A1,SLC2A4,SORD,UCP3
HNF4A	transcription regulator	1.19E-10	ACAA2,ACAT1,Acot1,ACSL1,ACY1,ACY3,ALDH2,ALDH5A1,ALDOB,AMACR,AS3MT,BCKDHA,BCL6,BOLA1,C21orf33/LOC102724023,C3,C4orf27,Cdkn1c,CLPX,CMSS1,COQ3,CPT2,CRAT,CREBL2,CUTC,CUX2,DBP,DBT,DEDD2,DHRS4,DNAJC28,DTWD1,ETFDH,FBXO31,FGF13,FYCO1,GCHFR,GFM1,GOT1,GPT,GRB14,GSTK1,GTF2H4,HADHA,HADHB,HSD11B1,HSPE1,HSPH1,IL15,KCNJ12,KIAA0141,KLF15,L2HGDH,LARS2,MCCC1,MCEE,MGST1,MID1IP1,MIPEP,MLXIPL,MRPS21,MSRB2,MUT,NAMPT,NARS2,NDUFA5,NDUFS1,NUDT6,PANK1,PDSS2,PEX6,PFDN6,PHB,PINK1,PNPO,PPARA,PPFIBP2,PPIL1,PPIP5K2,PPL,PRDX5,RMND1,RPAP3,RPS6KA5,RTN4IP1,SCAND1,SLC22A3,SLC25A13,SLC25A20,SQRDL,STARD10,SUCLA2,SUCLG1,TBC1D16,TEF,TFPT,TMEM126B,UPF3B,UQCC1,UROS
INSR	kinase	3.99E-10	ACAA2,ACADM,ACADVL,ACOT2,ACSL1,ALDH2,ALDH6A1,ATP5G1,CPT2,CRAT,DECR1,ECI1,ETFA,ETFB,ETFDH,FDFT1,GADD45A,HADHA,HADHB,HSPD1,IDH1,KLF9,MRPS21,NAMPT,PFDN6,PPARA,PRKCQ,RTN2,SLC25A20,SLC2A4,SUCLA2,UCP3
PPARD	ligand-dependent nuclear receptor	6.48E-09	ACAA2,ACADVL,ACSL6,ACY1,ALDH2,Cdkn1c,CPT2,ECH1,HMGCS2,LDHB,LGALS4,MLYCD,Pcp4l1,PNPLA2,SLC22A3,SLC25A20,SLC27A1,SLC2A4,SORD,TCEA3,UCP3
PPARGC1A	transcription regulator	1.13E-08	ACACB,ACADM,ACADVL,ACAT1,C3,FBXO32,FNDC5,MAL,MAOB,MT-CO2,NDUFS1,PLIN5,PNPLA2,PPARA,PRDX5,SDHA,SLC25A20,SLC2A4,SOD2,UCP3
PRKAG3	kinase	1.26E-08	ACSL6,AMD1,Cdkn1c,CES1,CLCN3,COQ3,GID4,GOT1,IL15,JPH1,MAGIX,MAP2K6,METTL7A,MID1IP1,NAMPT,SLC40A1,SLC4A3,SORD,THRSP,WNK2
HTT	transcription regulator	2.12E-08	ACADM,ACOT2,AMACR,AMD1,ATP2A2,ATP5G1,ATPAF1,BCL6,CAMK2A,CAMK2B,CITED2,DBP,ECI1,ENO3,ENPP2,FDFT1,FKBP4,HSPD1,HSPE1,IFI16,IL15,KCNIP2,KCNJ12,KCNJ2,KCNK3,KLF9,LDHB,NDUFA12,NDUFA5,NDUFS7,PENK,PER2,PPARA,RPS6KA5,RXRG,SCN4B,SDHA,SLC25A22,SLC40A1,SOD2,TESC,THRB,THRSP,TUBA4A,UQCR11
PPARG	ligand-dependent nuclear receptor	2.82E-08	ACAA2,ACADM,ACSL1,ATP2A2,BCL6,C3,Cdkn1c,CES1,CFD,CPT2,CRAT,CXCL14,DGAT2,EHHADH,FBP2,GPT,HADHA,HADHB,HMGCS2,IVD,LOC102724788/PRODH,MGST1,MLYCD,NDUFA5,PEX11A,PEX6,PLIN5,PPARA,SLC25A20,SLC27A1,SLC2A4,UCP3

A

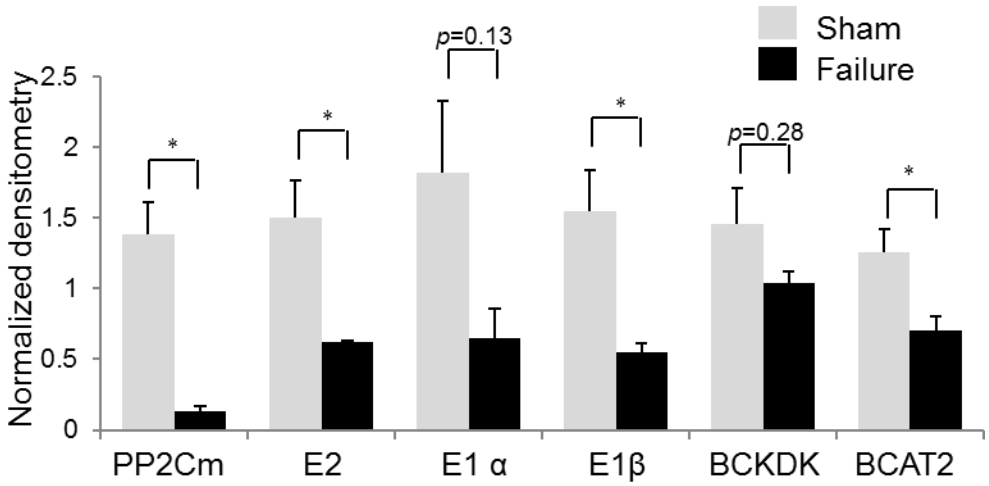

B

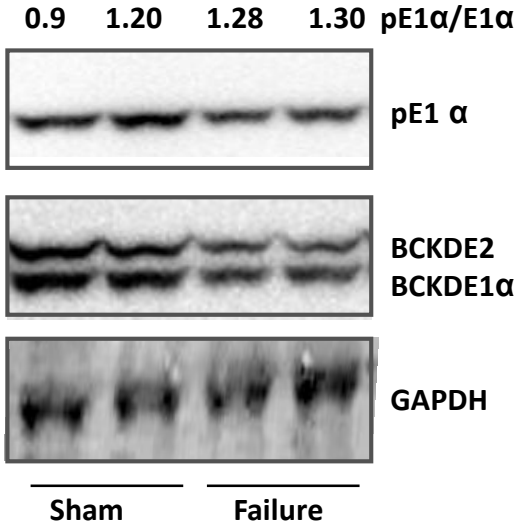

Supplemental Figure S1

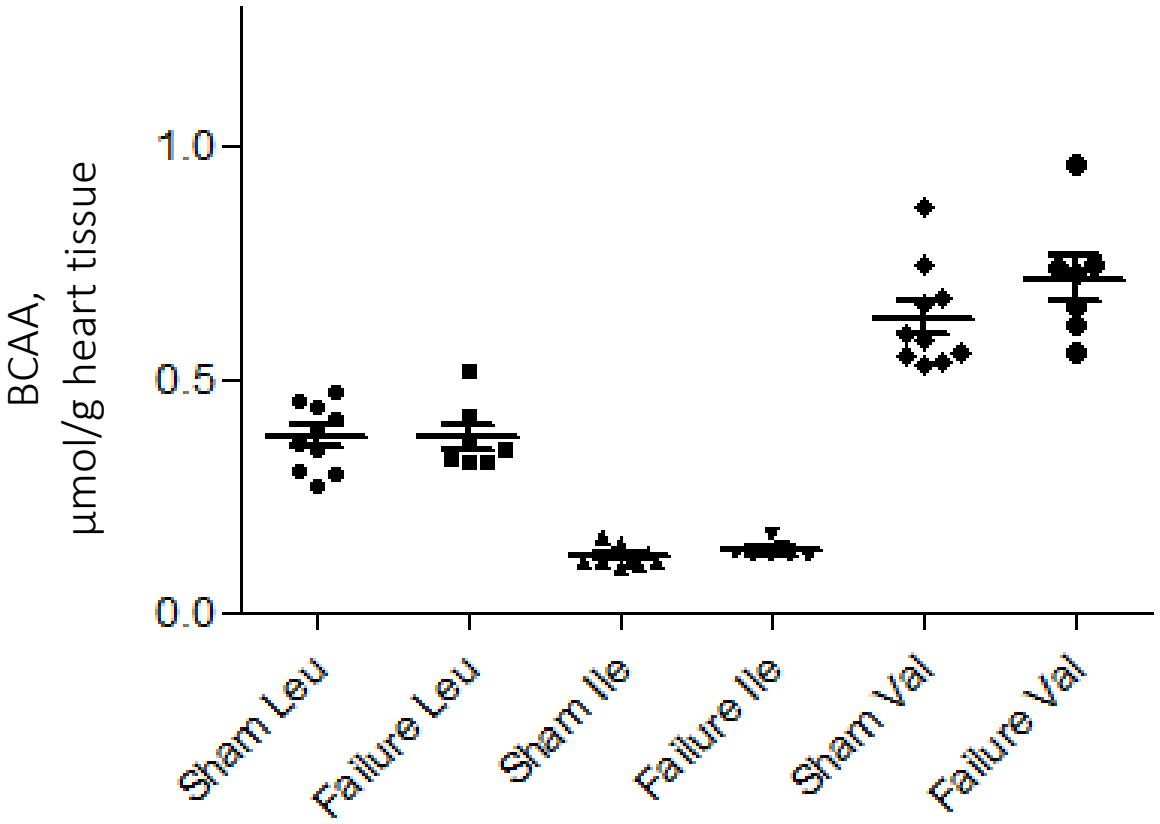

Supplemental Figure S2.

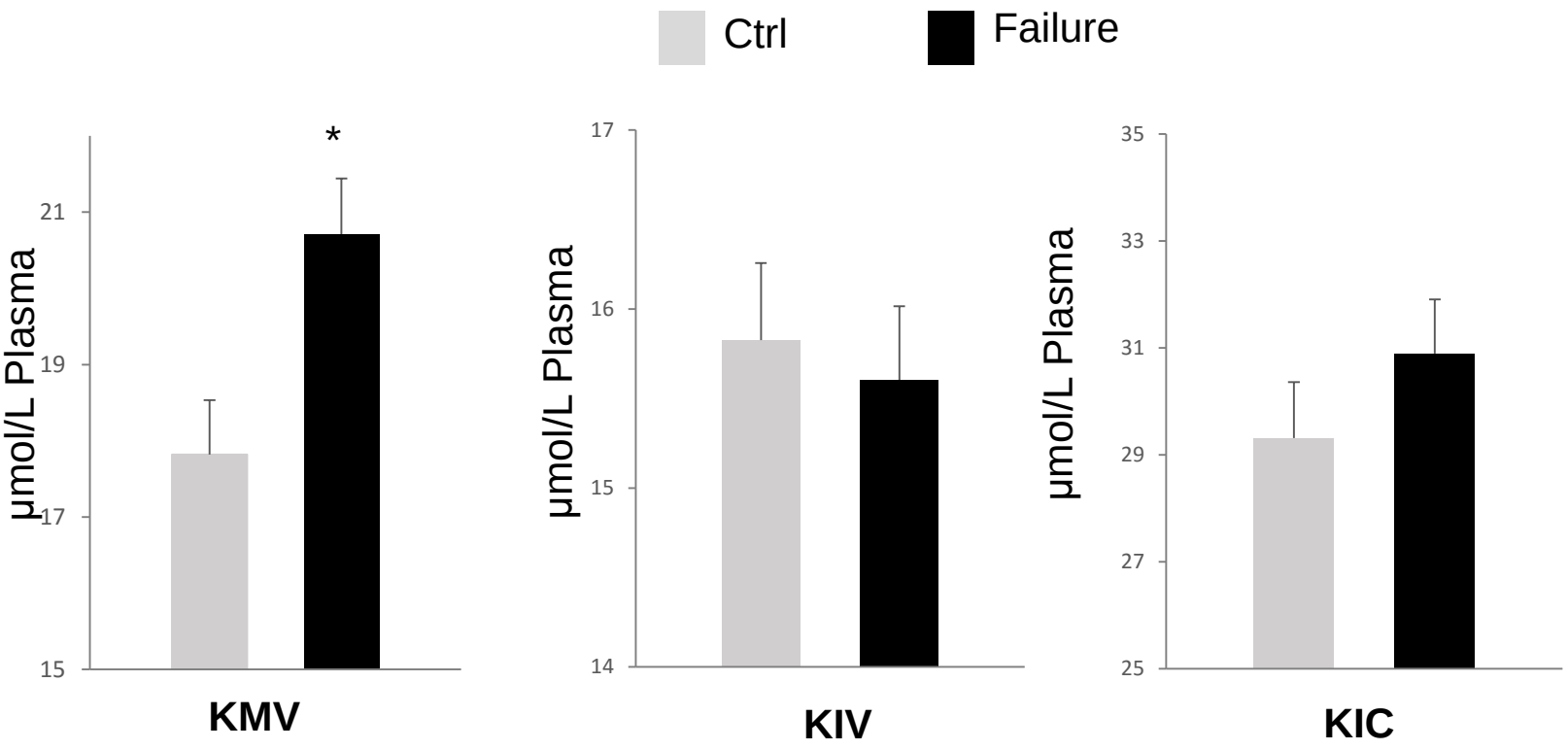

Supplemental Figure S3.

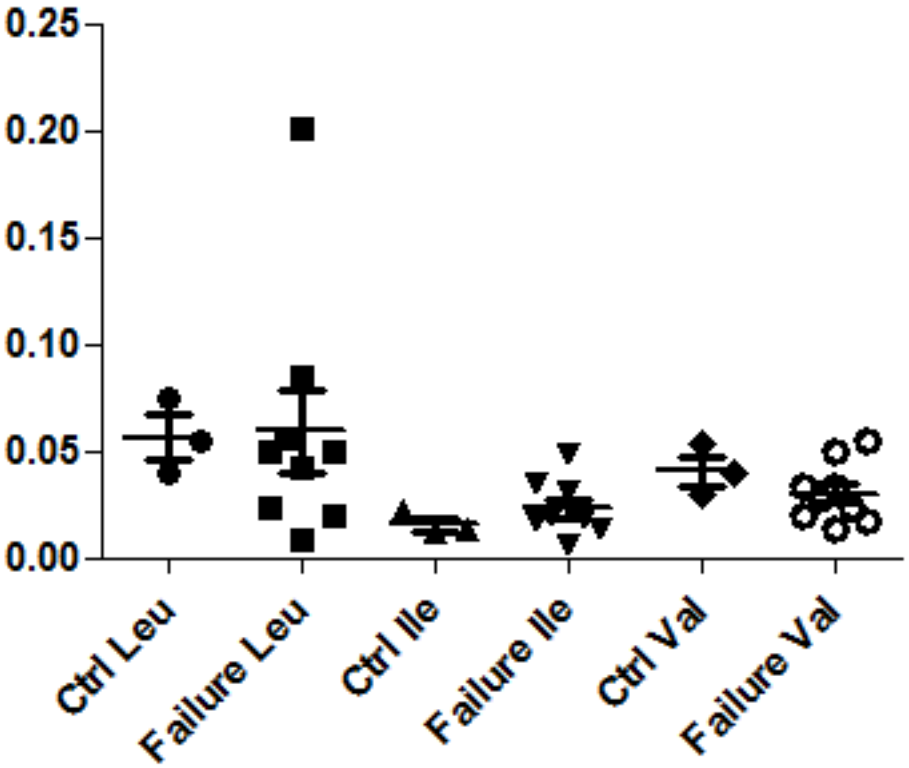

Supplemental Figure S4.

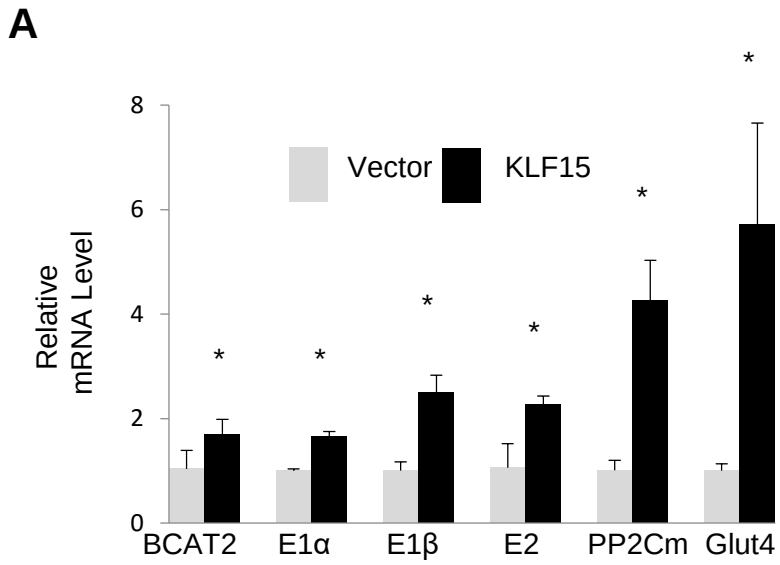

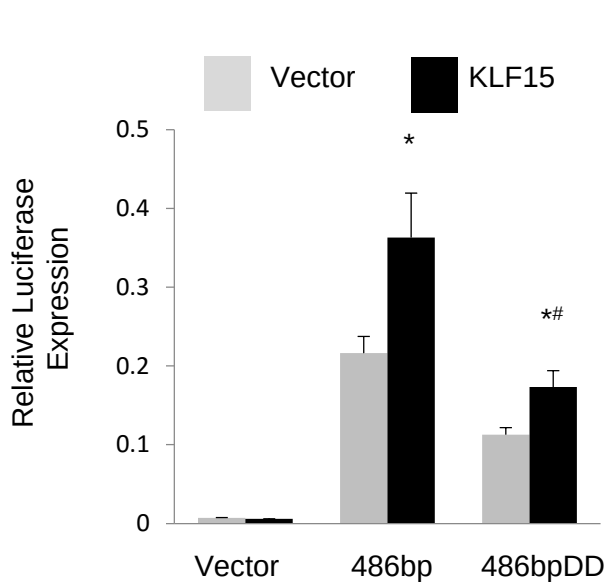

Supplemental Figure S5

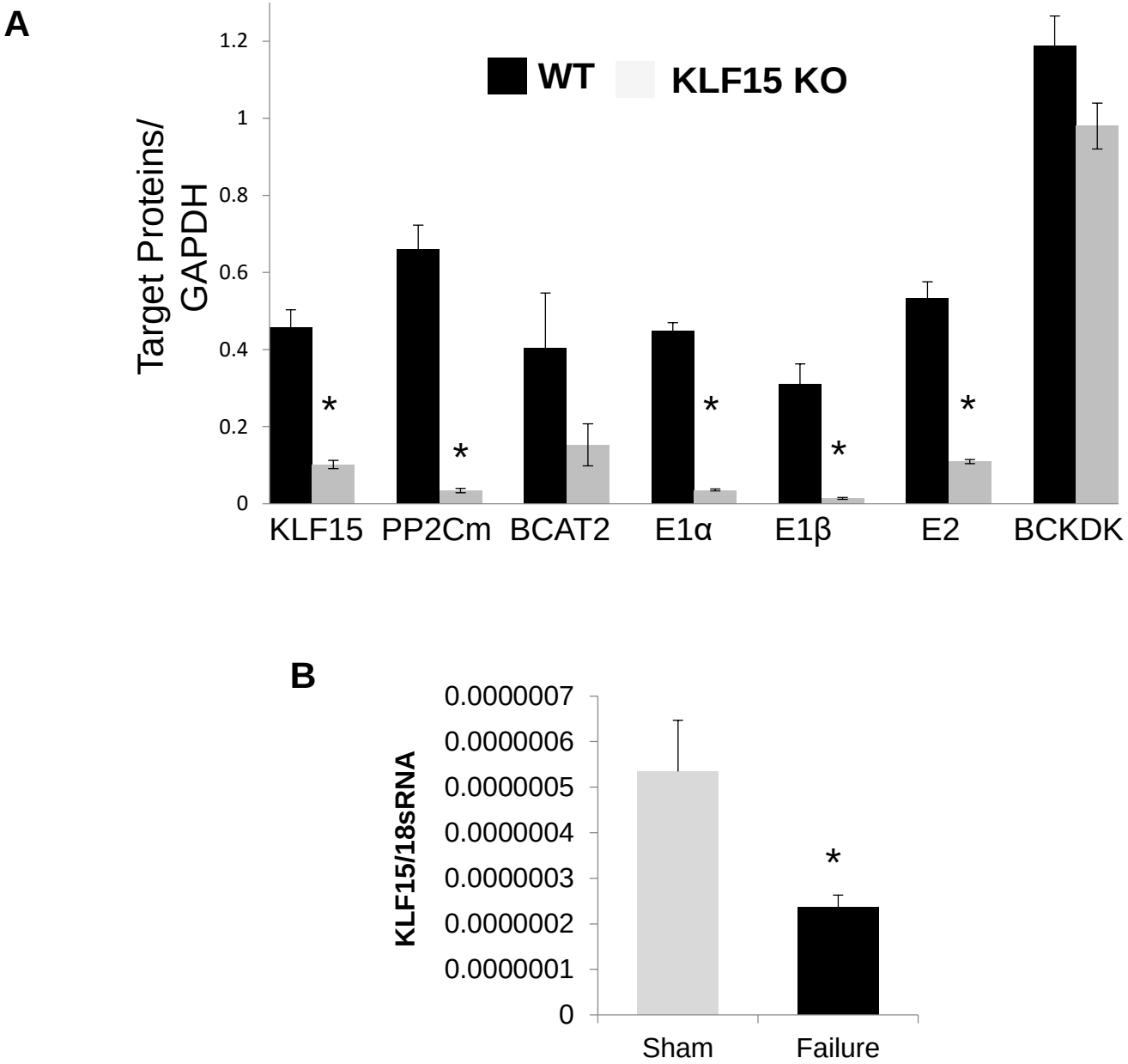

Supplemental Figure S6.

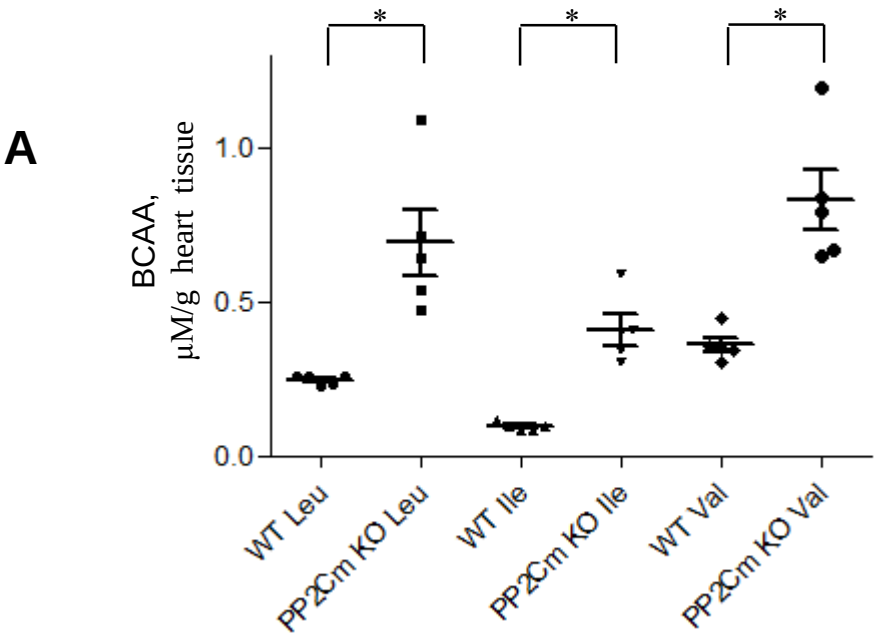

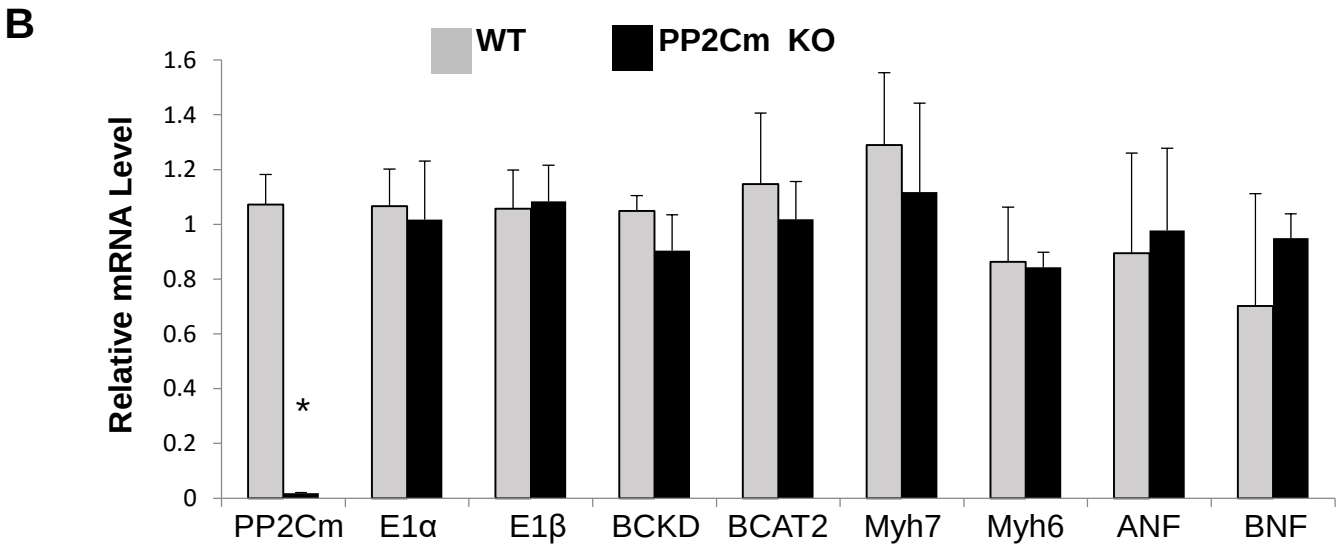

Supplemental Figure S7.

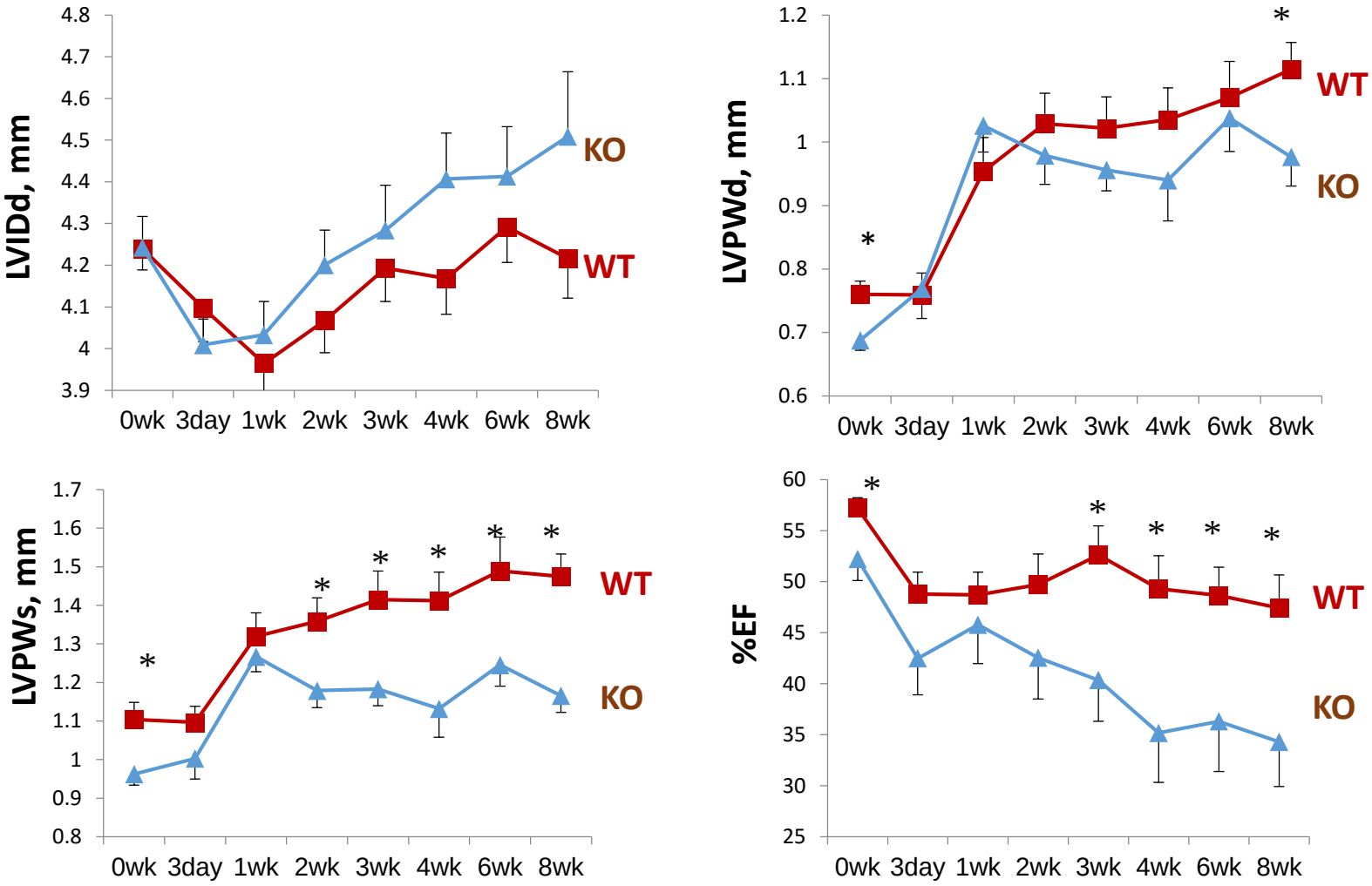

Supplemental Figure S8.

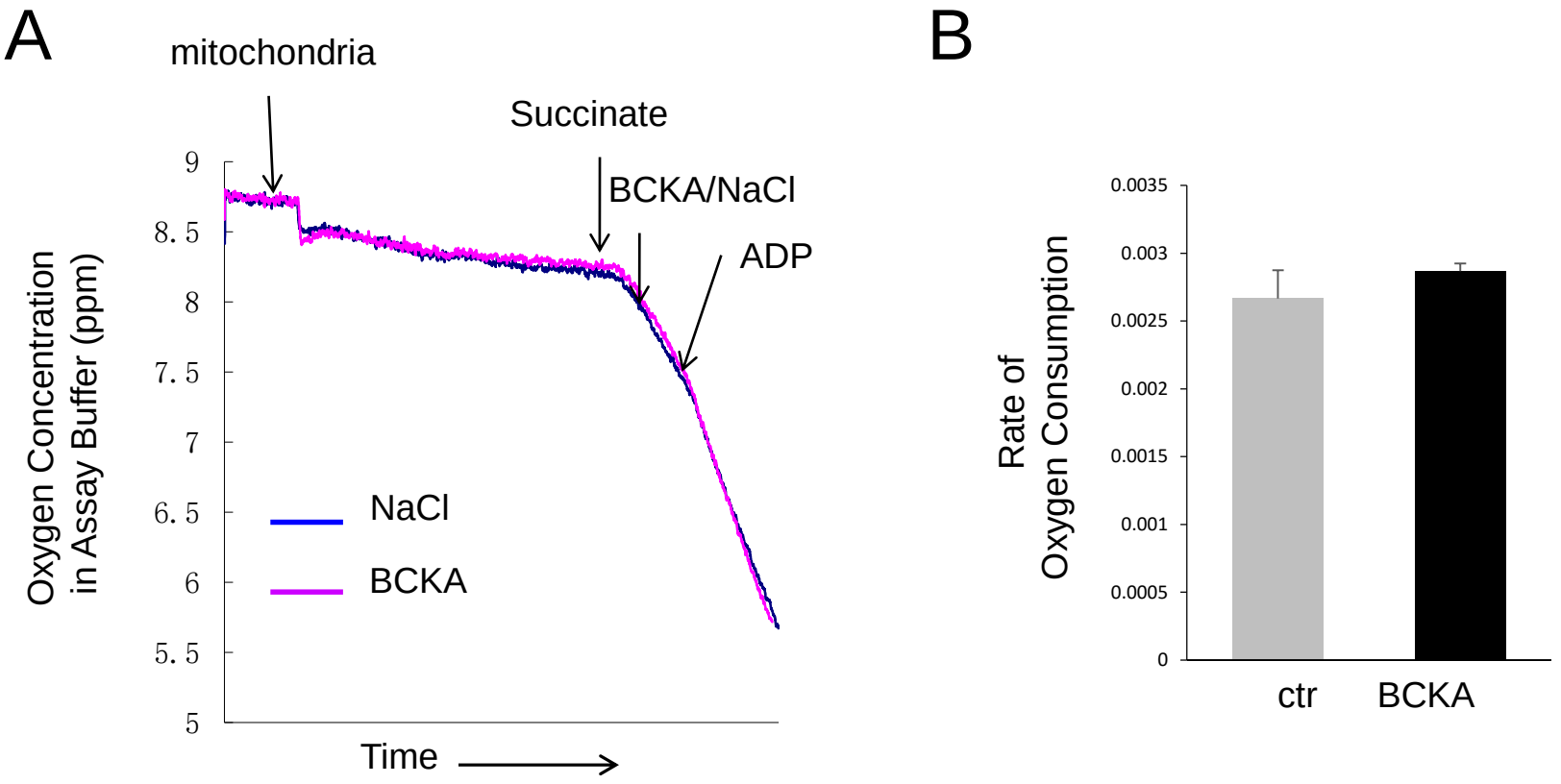

Supplemental Figure S9.

A

Actual Group \ Predicted Group	KO	WT	Class Error
KO	7	0	0.000
WT	0	8	0.000
Predictive accuracy = 100%			

B

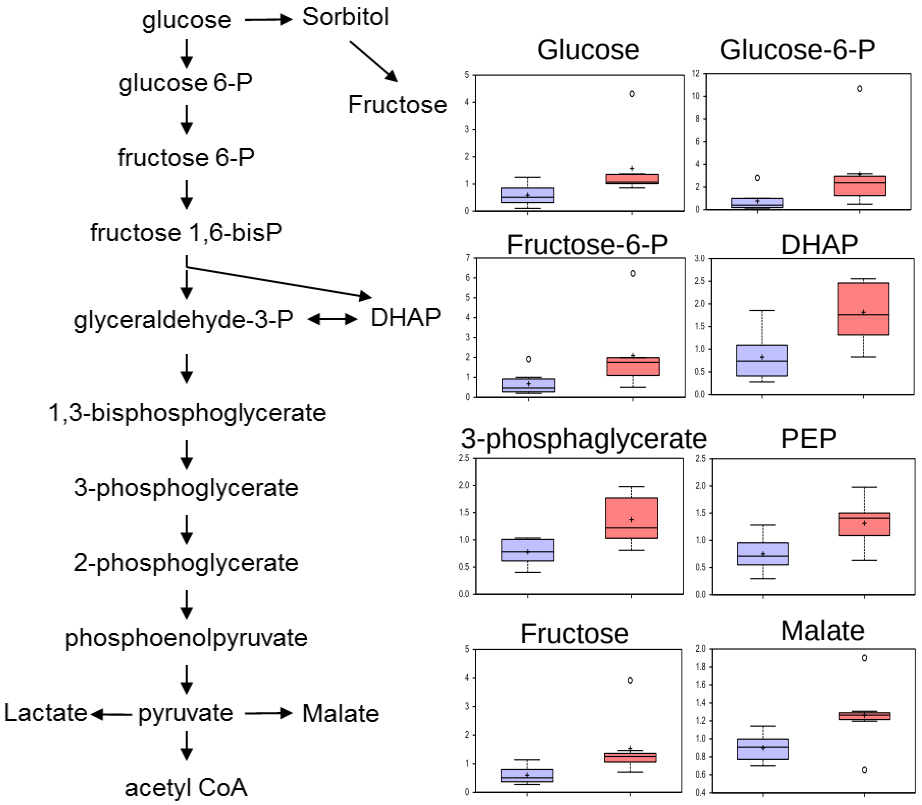

Supplemental Figure S10.

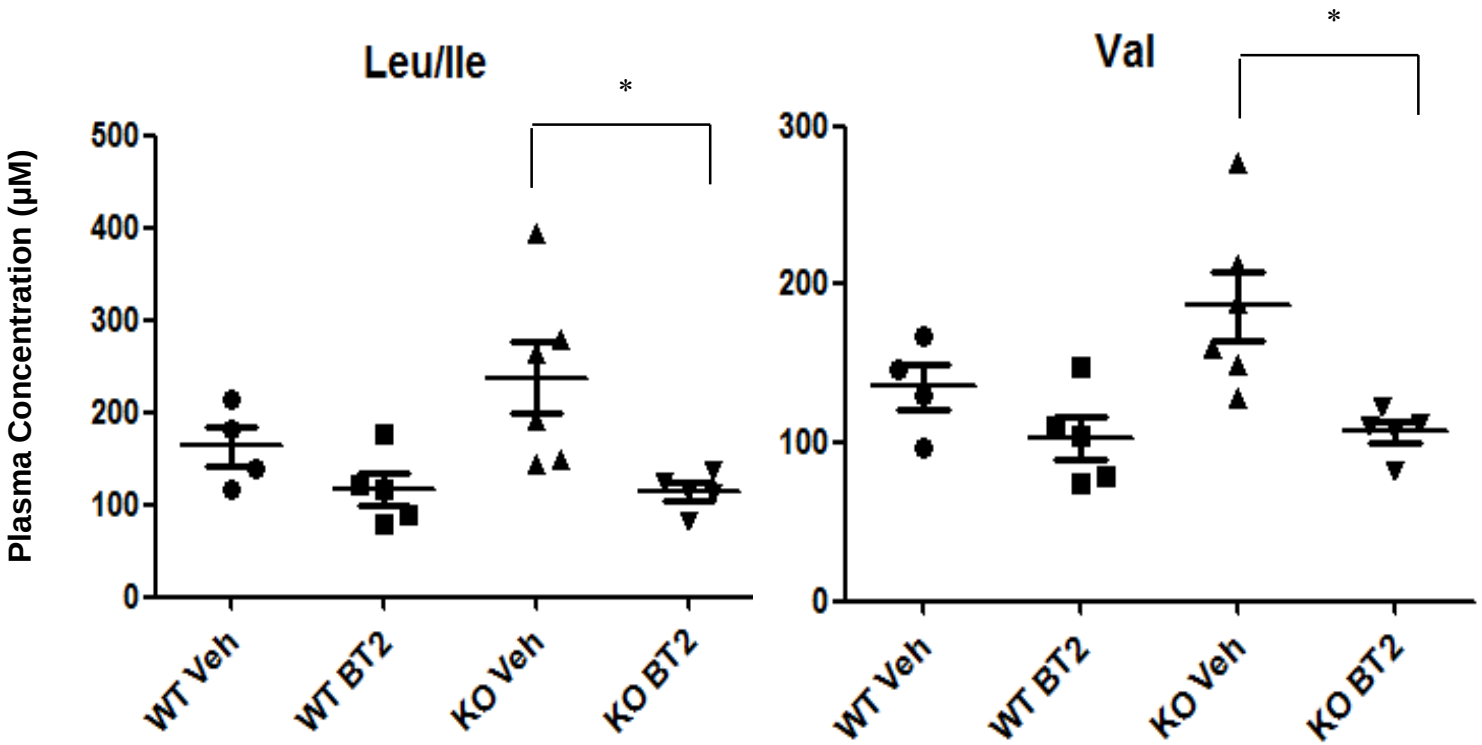

Supplemental Figure S11.

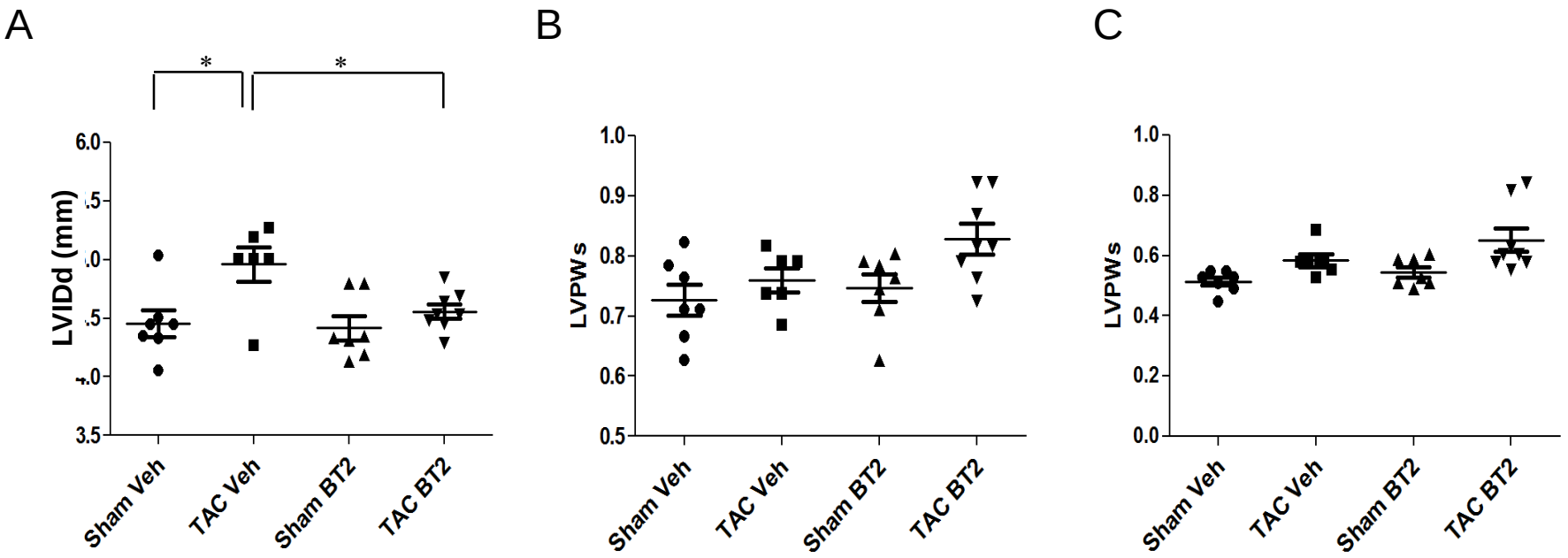

Supplemental Figure S12.